CERN 72-11
Laboratory I
Track Chambers
Division
4 July 1972

ORGANISATION EUROPÉENNE POUR LA RECHERCHE NUCLÉAIRE
CERN EUROPEAN ORGANIZATION FOR NUCLEAR RESEARCH

THE CERN MAGNETIC HORN (1971) AND ITS REMOTE-HANDLING SYSTEM

J.C. Dusseux, J.B.M. Pattison and G. Ziebarth

G E N E V A

1972

CERN 72-11
Laboratory I
Track Chambers
Division
4 July 1972

ORGANISATION EUROPÉENNE POUR LA RECHERCHE NUCLÉAIRE
CERN EUROPEAN ORGANIZATION FOR NUCLEAR RESEARCH

THE CERN MAGNETIC HORN (1971) AND ITS REMOTE-HANDLING SYSTEM

J.C. Dusseux, J.B.M. Pattison and G. Ziebarth*)

G E N E V A

1972

*) Present address: Thyssen-Niederrhein, 42-Oberhausen, Germany.

CERN - Service d'Information scientifique - H/505 - 1200 - juillet 1972

CONTENTS

1. INTRODUCTION AND MAIN FEATURE OF THE HORN SYSTEM, 1971

Since the first installation of the magnetic horn focusing device[1,2] in the CERN neutrino beam facility[3], considerable improvements have been made with respect to the optical performance as well as to the technical reliability of the system.

The neutrino beam facility (Fig. 1) now consists of the following:

i) A pulsed primary beam transport system which focuses the protons (typical momentum, 26 GeV/c) with an image size of ∿ 2.5 mm × 2.5 mm on a 90 cm long Be target.

ii) A more powerful magnetic horn of improved design partly surrounding the target, focuses the pions and kaons from the target into a nearly parallel beam. The horn, which is remotely interchangeable with two spare horns, is connected via a 13 m long "stripline" in series with 26 high-voltage/high-current coaxial cables to a 260 kJ (12 kV, 500 kA) capacitor bank[4].

iii) The secondary beam is focused again by two pulsed toroidal lenses ("reflectors" R2 and R3)[5].

iv) This beam, consisting also of the pion and kaon decay products (neutrinos and muons), is filtered by a 22 m long iron shield, whose distance from the target is 70 m ("decay path" for pions and kaons), so that only the neutrinos can pass into the heavy-liquid bubble chamber Gargamelle, which has a useful diameter of 1.60 m and serves as the detector for neutrino interactions.

Compared with the previous set-up, the improvements are essentially:

- an increase in the angular and momentum acceptance of the magnetic horn by a properly calculated horn shape using stronger focusing power;
- a minimization of particle absorption by reducing to a minimum the wall thickness of the horn inner conductor;
- a remote-handling system allowing a rapid and semi-automatic replacement of the horn in case of a failure;
- avoidance of radiation damage of the power coaxial cables and their connectors by means of a sandwich-like two-conductor stripline system;
- the possibility of quick change from focusing of neutrinos to antineutrinos by means of an automatic polarity changer for the horn current;
- a vibration-free and remotely inclinable suspension of the target;
- additional monitoring systems for centring the incoming proton beam, for measuring the magnetic field strength in the horn, and for checking the orientation of horn and target.

2. HORN INNER CONDUCTOR

2.1 Optical design

As the magnetic horn enhances the neutrino flux in the detector volume by a factor of approximately 20, a careful design of its optical properties is indispensable for obtaining an intense neutrino beam.

The computer program NUFLUX[6] calculates the trajectories of the neutrino parent particles (pions and kaons) in the azimuthal magnetic field B (kG) confined between the inner and the outer conductors of the coaxial horn (Fig. 2):

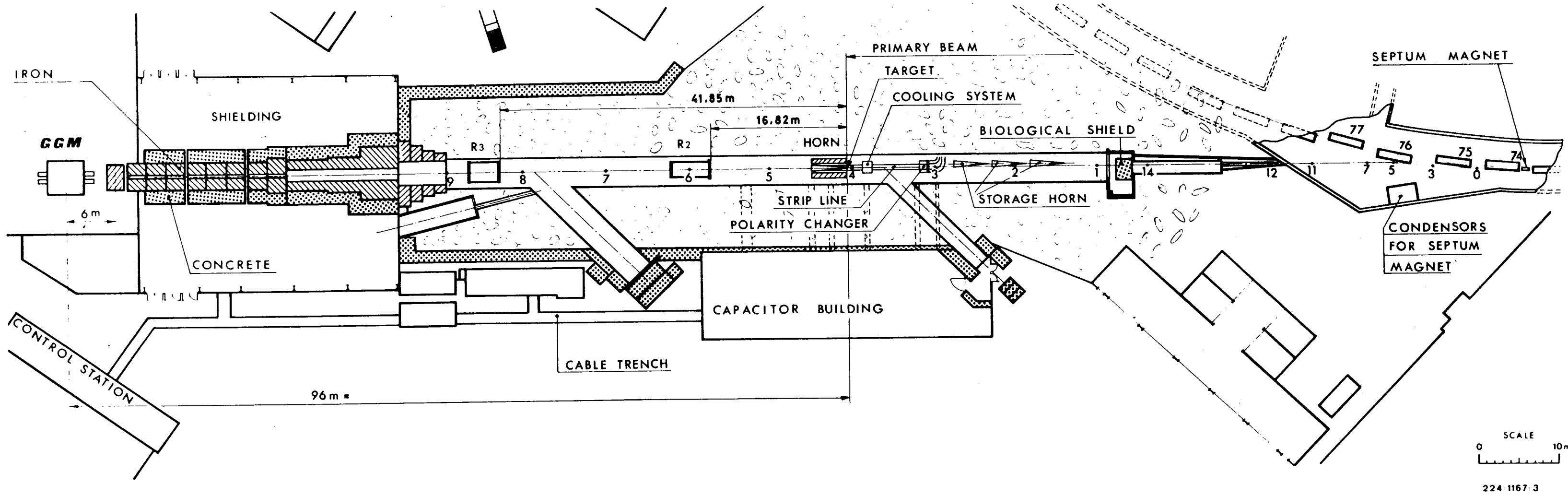

Fig. 1 Neutrino beam

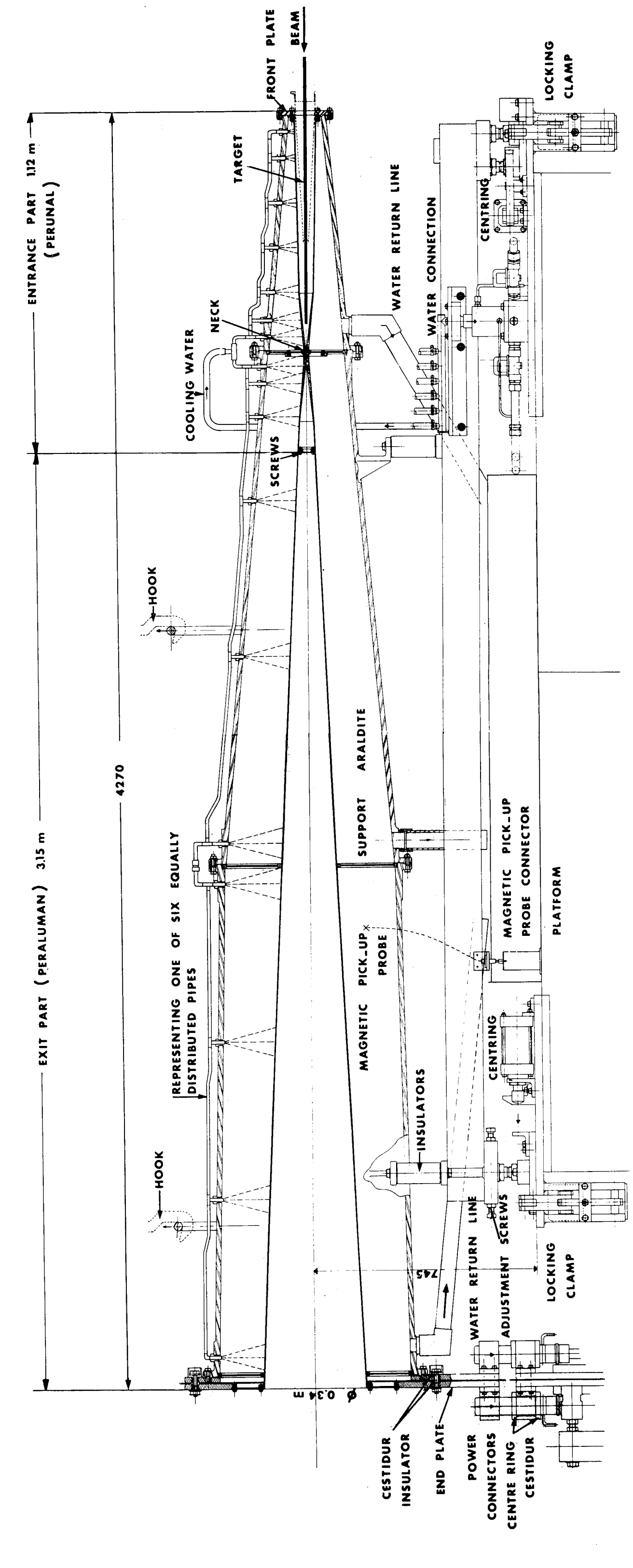

Fig. 2 Magnetic horn

$$B(r) = 0.2 \frac{I}{r} , \quad (1)$$

where I (kA) is the current flowing through the horn, and r (cm) is the radial distance from the horn axis. As the shape of the outer conductor is made large enough not to interfere with the particle trajectories, the optical properties of the horn are determined solely by the horn current and the shape of the inner conductor. The latter is calculated for incoming particles of a selected momentum range and of entrance angles up to ∿ 110 mrad, in such a way that the particles leave the horn as an approximately parallel beam.

The present horn is 4.3 m long and has a long conical entry surface (as opposed to a cylinder in earlier horns) partially surrounding the target. A further small improvement could have been obtained by making the exit diameter larger. This was not possible because of space restrictions in the neutrino tunnel.

By a lengthy optimization procedure[7]), the best set of values for horn and reflector currents I, and for distances X between target front end and focusing elements, was found using again the NUFLUX program.

For 26 GeV/c proton momentum, the optimum parameters are:

$$I_{horn} = 340 \text{ kA} , \quad I_{R2} = 400 \text{ kA} , \quad I_{R3} = 400 \text{ kA}$$

$$X_{horn} = 0.2 \text{ m} , \quad X_{R2} = 16.6 \text{ m} , \quad X_{R3} \simeq 43.0 \text{ m}$$

giving a neutrino energy spectrum peaking at 2-3 GeV (Table 1).

TABLE 1

Neutrino flux enhancement by horn and/or reflectors

Neutrino energy E_ν (GeV)	Enhancement of neutrino flux by a factor of		
	Horn only	Horn + reflectors R2, R3	R2, R3 only
1.0	16.0	32.0	5.6
2.0	26.0	81.0	13.2
3.0	45.0	67.0	11.4
4.0	21.0	25.0	4.1
5.0	10.0	13.0	2.7
6.0	6.0	8.5	2.1
7.0	8.5	11.0	2.5
8.0	12.0	14.5	3.2
9.0	20.0	24.0	4.0
10.0	17.0	23.0	5.2

Proton momentum: 26 GeV/c (pion and kaon production spectrum as given by the "Thermodynamical Model").
I_{horn} = 340 kA, I_{R2} = I_{R3} = 400 kA
X_{horn} = 0.17 m, X_{R2} = 16.7 m, X_{R3} = 43.0 m (from target front end).

2.2 Mechanical design

The particle absorption loss in the horn material is considerable (∿ 15%), owing to the small angles of the particle trajectories relative to the inner-conductor walls, though the mean free path of pions and kaons in the conductor material (aluminium) is rather large: $\lambda \simeq 0.4$ m.

Thus a minimization of the wall thickness is very important in order to gain neutrino intensity. The minimum wall thickness necessary to withstand the mechanical stress caused by the current forces has been calculated by the computer program HORN[8]) for each section of the inner conductor. This program considers the conductor as consisting of 23 sections (mostly conical) of mass m_i, length ℓ_i, inner radii R_i, R_{i+1} and outer radii R_i', R_{i+1}'. The sections are coupled together by the elasticity c_i of the material. The forces F_i exerted on this dynamical system during the current pulse $I(t) = I_0 \cdot \sin \omega t$ are due to the effect of the magnet field $B(r,t)$ -- created by the current -- upon the current itself in the conductor wall:

$$F_i = \int dF_i = \int I\, B_i\, d\ell_i = 0.2 \int_0^{\ell_i} \frac{I^2}{r_i}\, d\ell_i = 0.2 \frac{1}{\mathrm{tg}\, \alpha_i} \int_{R_i'}^{R_{i+1}'} \frac{I^2}{r_i}\, dr_i = \frac{0.2\, \ell_i}{R_{i+1}' - R_i'}\, I^2 \ln \frac{R_{i+1}'}{R_i'} \quad , \tag{2}$$

where F_i is measured in Newton (≈ 0.1 kp) and α_i is the cone angle, for which we have

$$\mathrm{tg}\, \alpha_i = \frac{R_{i+1}' - R_i'}{\ell_i} \quad .$$

For a cylindrical section, Eq. (2) becomes

$$F_i = 0.2 \frac{I^2}{R_i'}\, \ell_i \quad . \tag{2a}$$

We shall denote the axial component (i.e. in x-direction) of F by F_{ax}:

$$F_{ax,i} = F_i \sin \alpha_i = F_i \frac{\mathrm{tg}\, \alpha_i}{\sqrt{1 + \mathrm{tg}^2\, \alpha_i}} \quad . \tag{3}$$

The elasticity factor c_i between two sections is defined by Hook's law:

$$F_{ax,i} = E\, Q_i \frac{\Delta \ell_i}{\ell_i} = c_i\, \Delta \ell_i \quad , \tag{4}$$

where E = Young's modulus of elasticity, characterizing the material, and Q_i = cross-section area of section i. For a conical or cylindrical section, we get from Eq. (4):

$$c_i = \frac{\pi E}{3 \ell_i} \left[(R_{i+1}' + R_i')^2 - (R_{i+1} + R_i)^2 - R_i' R_{i+1}' + R_i R_{i+1} \right] \quad . \tag{4a}$$

The mass m_i is completely described by the size of the section and the material density ρ. It can be expressed in terms of c_i:

$$m_i = \frac{\rho}{E} \ell_i^2\, c_i \quad . \tag{5}$$

The equation of motion describing the forced oscillation of the dynamical system in the axial direction is:

$$m_i \frac{d^2x_i}{dt^2} = c_i(x_{i-1} - x_i) + c_{i+1}(x_{i+1} - x_i) + F_{ax,i}(t) \quad \text{for} \quad 2 \le i \le 22 \ . \tag{6}$$

As boundary condition we have for the first and last sections:

$$m_1 \frac{dx_1^2}{dt^2} = 0 \quad \text{(i.e. clamped)} \tag{6a}$$

$$m_{23} \frac{dx_{23}^2}{dt^2} = 0 \quad \text{(i.e. free moving since } C_{23} = 0) \tag{6b}$$

This system of 23 inhomogeneous differential equations of second order is solved in the program HORN by a Runge-Kutta step-by-step integration method after transformation into a system of 46 differential equations of first order, using as initial conditions:

$$x_i(t = 0) = 0 \ ; \quad \frac{dx_i}{dt}(t = 0) = 0 \qquad \text{(i.e. no motion at the beginning of the current pulse)}$$

$$F_{ax,i} = 0 \quad \text{for} \quad t > {}^T\!/2 \ , \quad \text{where} \quad {}^T\!/2 = 230 \ \mu\text{sec} \quad = \text{half pulse length (ideal, i.e. damping neglected)}$$

The resulting amplitudes $x_i(t)$ are used for calculating the mechanical stress $\sigma_i = F_{ax,i}/Q_i$ according to Eq. (4), so that

$$\sigma_i = c_i \frac{\Delta \ell_i}{Q_i} = \frac{c_i}{Q_i}(x_{i-1} - x_i) \ . \tag{7}$$

The wall thickness is now adjusted in such a way that the stress on each section does not exceed the stress-limit σ_{limit} for the material, quoted in Table 2; σ_i is typically ≤ 1.8 ton/cm^2 at I = 400 kA.

Less important than this axial component of the stress is the radial stress. Only for sections where the radius is bigger than 4 cm does the radial force require more wall thickness than the axial one. This is also calculated in program HORN in a quasi-static way by comparing the magnetic pressure on the material with experimentally known pressure limits[9]) for compressing seamless pipes of the same material and radius, taking into account an estimated time-compensating factor[8]).

The minimum wall thickness of cylindrical Al alloy sections required to withstand the radial component of the magnetic force is approximately given by:

$$(R_i' - R_i)_{min,\,Al} \simeq 7 \times 10^{-5} \sqrt[3]{R_i'^2 \, I_0^2} \ (R', R \text{ in m, } I_0 \text{ in kA}) \ . \tag{8}$$

The horn inner conductor (Fig. 3) is made out of two different Al alloys, whose characteristics are listed in Table 2. The entrance part, comprising the "target part" and the very narrow "neck" region, is made from Perunal. This part is subject to very high axial stress, especially in the neck region; therefore the alloy having the highest σ_{limit} has been used.

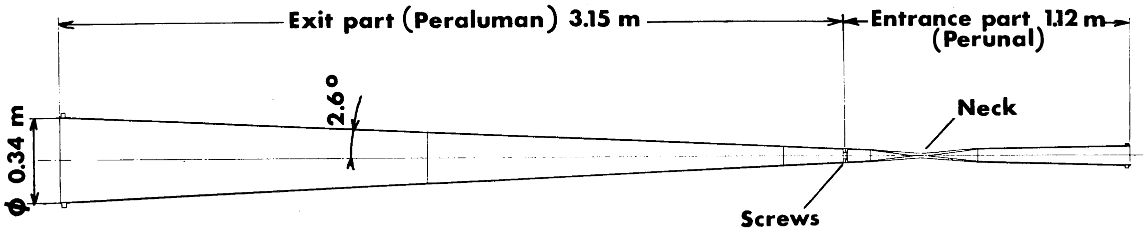

Fig. 3 Inner conductor

TABLE 2

Properties of inner conductor material

	Symbol	Perunal (entrance part)	Peraluman-30 (exit part)	Units
Chemical composition:	Cu	1.3-1.8	0.05 max	%
	Si	+Fe: 0.4 max	0.4 max	%
	Mn	0.1-0.4	0.1-0.5	%
	Mg	2.1-2.5	2.6-3.1	%
Aluminium +	Zn	6.0-6.5	0.1 max	%
	Fe		0.3 max	%
	Cr	0.1-0.3	-	%
	Ti	0.03-0.15	-	%
Young's modulus of elasticity	E	7,000	6,300	kp/mm^2
Density	ρ	2.85	2.65	g/cm^3
Mechanical stress limit for 2 × 10^6 alternate tractions (not guaranteed by manufacturer)	σ_{limit}	18-20	14	kp/mm^2
Specific electrical resistance	κ_{spec}	55	47	$m\Omega \cdot mm^2/m$

Conversion into the units used in the equation is done by:

$1\ kp/mm^2 \simeq 10^7\ N/m^2$.

The radial force is important only in the exit part of the inner conductor where the comparatively weak axial stress allows a wider choice of materials. Peraluman-30 has been chosen mainly for its good welding characteristics and because it is best suited for sheet-metal working.

3. CONSTRUCTION OF THE HORN

3.1 Inner conductor

In order to avoid additional particle absorption by screwed joints, the entrance part of the inner conductor has been manufactured on a lathe in one single piece. The exit part is made by sheet-metal working and consists of three pieces which were argon-welded. The welding procedure necessitates a greater minimum wall thickness in certain parts than is required from the stress calculation[10].

The exit and entrance parts are screwed together, excellent electrical contact being assured by a 100 μm thick silver foil.

The (calculated and actual) dimensions of each conductor section are listed in Table 3.

TABLE 3

Dimensions of inner horn conductor

Section-number i	Length ℓ_i [cm] of section	Outer radius R_i [cm]		Wall thickness [≈ (R_i' - R_i)] [mm]				
				"400 kA horn-version"		"340 kA horn-version"		
		400 kA	340 kA	Calculated	Actual	Calculated	Actual	
1	0.1	3.8	3.73	1.5	2.2	0.8	1.0	Entrance part (Perunal)
2	8	3.6	3.53	1.5	2.2	0.8	1.0	
3	12	3.5	3.43	1.5	2.2	0.8	1.0	
4	30	2.85	2.78	1.4	2.2	0.9	1.0	
5	17	2.5	2.43	1.3	2.2	0.9	1.0	
6	9	1.6	1.55	3.8	4.5	3.3	3.5	
7	9	0.89	0.7	7.0	7.4	5.3	5.5	
8	5	0.89	0.7	8.3	8.9	6.9	7.0	
9	10	1.6	1.58	2.5	2.6	1.5	1.6	
10	10	2.5	2.4	1.5	2.2	1.0	1.3	
11	20	3.4		1.5	1.8	1.0	1.8	Exit part (Peraluman-30)
12	20	4.3		1.6	2.0	1.1	2.0	
13	30	5.65		1.7	2.0	1.1	2.0	
14	30	7.0		1.8	2.0	1.2	2.0	
15	30	8.4		1.9	2.0	1.2	2.0	
16	30	9.7		1.9	2.0	1.2	2.0	
17	30	11.05		2.0	2.5	1.2	2.5	
18	30	12.4		2.1	2.5	1.3	2.5	
19	30	13.8		2.2	2.5	1.3	2.5	
20	30	15.15		2.3	2.5	1.3	2.5	
21	30	16.5		2.3	2.5	1.3	2.5	
22	10	17.1		2.3	2.5	1.3	2.5	
23	4	17.2		2.3	2.5	1.3	2.5	

3.2 Outer conductor

There are no special requirements concerning the minimum wall thickness or tensile strength of the outer conductor. It has been manufactured from cast aluminium (Silafont 1) in three pieces, the largest being a cylinder of 0.67 m diameter. The wall thickness is 18 mm.

The inner conductor is centred inside the outer conductor by means of two Araldite disks of 5 mm thickness, in which holes of 4 cm Ø have been drilled in order to minimize absorption loss without seriously reducing the mechanical strength. The optimum positions of the disks have been calculated by using program BENDVIB to minimize the vibration amplitudes of the inner conductor due to possible misalignments.

The outer conductor is equipped with a system of external pipes by which demineralized cooling water is sprayed onto the inner conductor immediately after the current pulse. The relative quantity of water at each horn section was pre-determined by program HORN, which calculates the adiabatic temperature rise due to the ohmic resistance of the conductor at the section surface. The temperature rise is maximum in the neck region (20°C per pulse) and minimum at the downstream end of the horn (0.1°C per pulse). The total amount of cooling water is 30 ℓ/min. It has been found that adding 0.5% of Wynn's machine oil to the water effectively prevents corrosion of the inner conductor.

Prior to the application, a sample of this oil had successfully passed a radiation acceptance test of 10^8 rad. The target end of the horn is made water-tight by means of a thick front plate and a 100 μm thick silver foil -- which also provides good electrical contact -- between the inner and outer conductors; the exit end is sealed by a conventional rubber O-ring.

A short piece of vertical "stripline" is connected at the downstream end of the horn. This end plate consists of two sandwiched aluminium plates of 20 mm thickness with a radiation-resistant insulator (2 mm thick Vetronite plus 2 × 3 Kapton*) sheets, each 125 μm thick) in between.

The force (P) per cm^2 between the end plates during the passage of the current pulse I (kA) is given by Eq. (9) [11] as an approximation for the case where the distance between the plates is much smaller than their width w (m):

$$P\left(kp/cm^2\right) = 6.3 \left(\frac{I}{w}\right)^2 . \tag{9}$$

For 400 kA pulsed current, P = 1.3 kp/cm^2 = 13 $tons/m^2$. Thus the plates had to be held together by insulated bolts placed every 16 cm, the insulation being obtained by sleeves made from highly radiation-resistant (> 10^9 rad) Cestidur**).

3.3 Chassis

The horn is mounted on an aluminium chassis having precisely machined base plates which are necessary for positioning the chassis on the platform in the beam by means of

---

*) Extremely radiation-resistant polymide (H-film) manufactured by Du Pont de Nemours (>> 10^9 rad).

**) Cestidur S.A., Lyon.

remote-controlled pneumatic pistons. Adjusting screws permit horizontal and vertical positioning of the horn relative to the chassis.

The connection between the chassis and the horn is done by three 15 cm long Araldite rods insulating the grounded chassis from the horn, which is at 10 kV potential during the current pulse.

The total weight of the horn and chassis is $\sim$ 500 kg; the remotely-controlled overhead crane can pick up and transport this unit by means of two hooks screwed onto the top of the outer conductor.

4. STRIPLINE AND POLARITY CHANGER

The old system of connecting the power-feed cables directly to the horn has been abandoned because experience has shown that the exposure of the HT cables to the ionizing radiation during neutrino runs results in heavy damage and can thus cause their explosion.

Therefore a "stripline" of 13 m length has been constructed. This is fairly insensitive to radiation damage, and is connected via special, remotely-controlled piston connectors to the end-plate of the horn. At the other end, the stripline is connected (via a polarity changer) to 26 parallel HT cables coming from the pulsed power supply.

The stripline consists of two aluminium plates of 35 cm width, sandwiched together with an intermediate insulating layer of 2 mm Vetronite plus 2 × 2 Mylar films of 125 μm thickness each. The electromagnetic force between the plates is given by Eq. (9): $P = 80$ tons/m^2 at 400 kA, which necessitates clamping by isolated U-profiles every 50 cm. The clamping is done in such a way that it does not prevent the stripline from expanding. The thermic expansion is estimated to $\sim$ 1.1 cm, although forced-air cooling is used. Open-air cooling is insufficient, as the stripline had to be covered by Vetronite in order to protect it from dust and water hazard, although radiation-resistant fibre-glass reinforced rubber hoses have been used in the water system to minimize the chances of such an accident occurring.

The polarity changer (Fig. 4) enables the operator to change the horn current polarity remotely within a minute after the current has been stopped. Basically, it interchanges two connection plates to the stripline by means of 10 pneumatically (8 atm) driven pistons of the same type as those described in the following section.

The polarity changer has been designed for a maximum of 500 kA, although the maximum current for the present horns is only 400 kA.

5. CONNECTION BETWEEN MOBILE AND FIXED INSTALLATION

5.1 Electric power connectors

The electrical connection between the stripline and the horn end plate is made by four sets of cylinder pairs and pistons, with an equivalent number for the return current. Each set comprises a hollow cylinder at the end of the stripline and the end plate, together with a piston pushed pneumatically into the cylinder. The electrical contact between the cylinders and the piston is accomplished by two laminated strips of silver-coated beryllium-bronze inside the silver-coated cylinder (Figs. 5 and 6). There are 75 "lamellae" on each

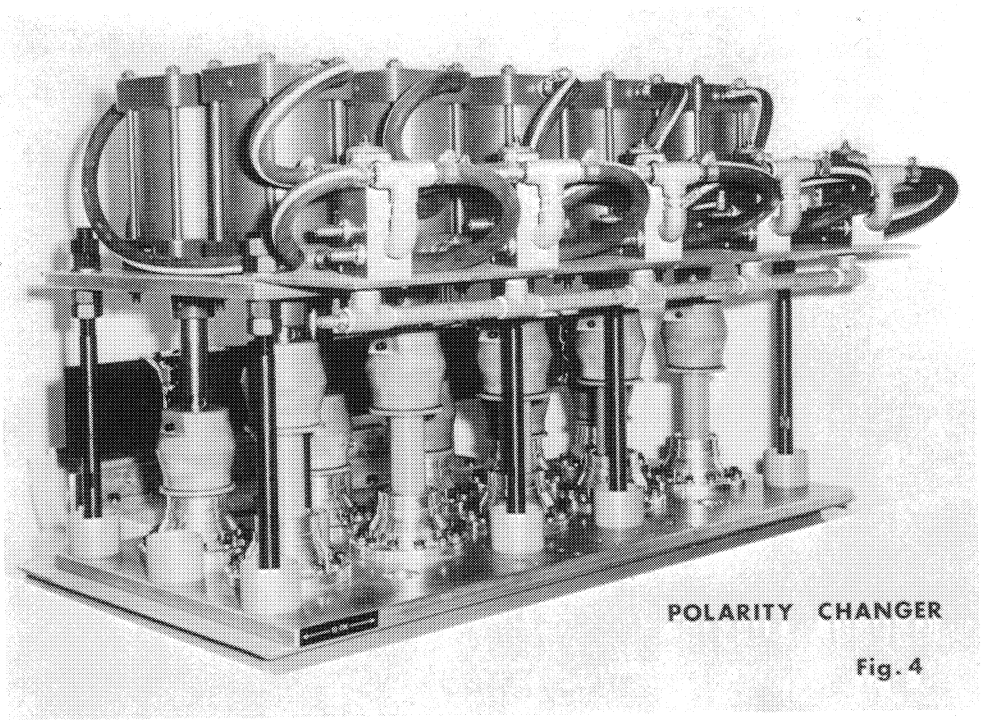

Fig. 4 Polarity changer

elastic Multicontact*) strip; each lamella has a thickness of 0.2 mm and an effective contact surface of 1.4 mm² and can transmit up to 20 A d.c. Since the lamellae have a tendency to scratch the surface of the piston in spite of the high elasticity of the strip, different surface coatings of the piston have been tried out: rhodium, tungsten, copper, silver sprayed on, and silver as a galvanic deposit. It has been found that a galvanic layer of 100 µm silver suits the purpose best, since it gives the optimum electrical contact and is sufficiently resistant to scratching.

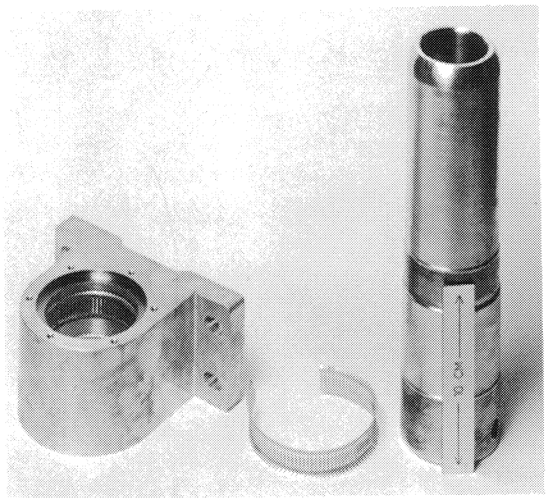

Fig. 5 Cylinder, lamella and piston (detail of Fig. 6)

The attractive electromagnetic force between two pistons of the same current direction is of the order of 140 kp, and the repulsive force between pistons of opposite current direction is ∿ 120 kp: owing to these forces and to the elasticity of the lamellae, the pistons move during a current pulse such that the electrical contact is not perfect everywhere, thus giving rise to high-voltage sparking which burns off the silver coating. This

*) Multicontact A.G., Basel.

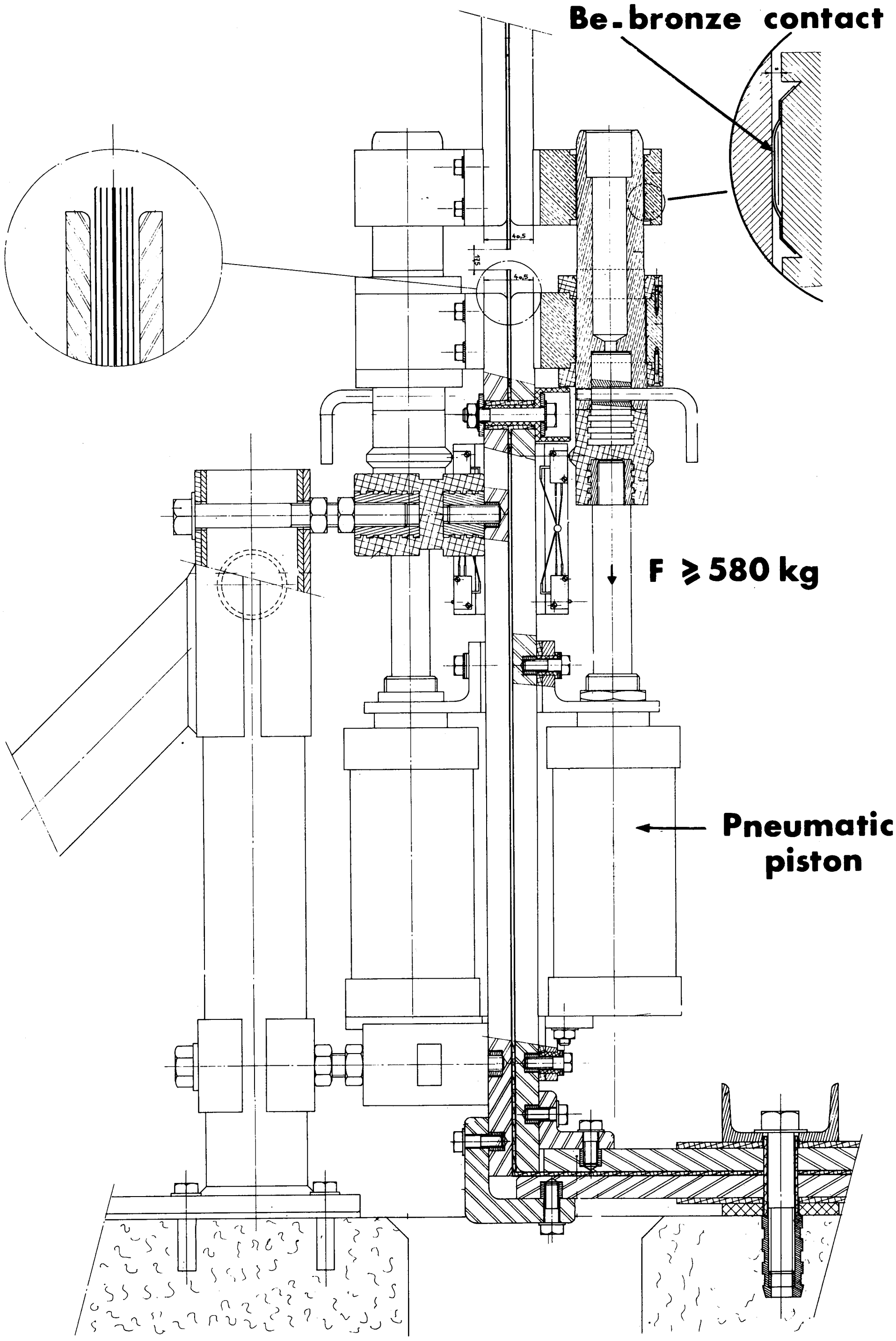

Fig. 6 Electric power connectors

effect could be prevented by blocking the piston mechanically in short Cestidur centre rings. Thus pulsed currents up to 180 kA have been transmitted in each current path during long endurance tests without visible damage to piston or lamellae.

5.2 Water connection

A spring-mounted hollow cylinder connects the water-cooling system and the horn. Disconnecting is done by compressed air; this has the advantage of avoiding flooding if the compressed-air system fails.

The electric isolation between the horn (on 10 kV potential during a current pulse) and the water-cooling system (ground potential) is accomplished by 40 cm long (radiation-resistant) rubber hoses*). They have an electric resistance of $R = 4 \times 10^9$ Ω/m, which is high compared to the resistance of the column of demineralized water in the system. When the water-connector is in the "disconnected" position, an interlock-switch automatically stops the cooling system and prevents an accidental switching-on.

5.3 Magnetic probe connector

The magnetic probe, installed in the horn and serving as a monitor for the magnetic field strength, is connected to the fixed installation (integrator, etc.) via a remotely commanded compressed-air piston which connects or disconnects a Lemo coaxial connector.

6. REMOTE EXCHANGE FACILITY FOR THE HORN

Owing to the minimized wall-thickness and the four welding lines of the inner horn conductor, the risk of breaking is not negligible. In a neutrino experiment, the environs of the magnetic horn have the highest radiation level in CERN: $\lesssim 5 \times 10^3$ roentgen/h during beam operation; $\lesssim 250$ roentgen/h at 7 min and $\lesssim 30$ roentgen/h at 1 h after beam stop. Therefore, manual exchange of the inner conductor in permissible time is excluded. A facility has therefore been constructed which permits the exchange of the complete horn assembly by means of a remotely handled overhead crane. The remote control is located in the neutrino control room, i.e. approximately 160 m from the neutrino tunnel. A pivoted television camera with a power-zoom lens and a microphone in the neutrino tunnel allow the operator in the control room to supervise visually and acoustically every step of the semi-automatic exchange procedure. Interlock switches serve as indicators for completed operation cycles and prevent the beginning of a new cycle prior to successful completion of the previous one. The procedure for changing a horn consists mainly of the following steps:

i) The mobile iron shielding around the horn, which serves as a biological shield for persons working near the neutrino tunnel, moves forward. It has a total weight of ∿ 100 tons and is mounted on a rail-carriage; its speed is 2 m/min. The crane with the TV camera attached, approaches the horn at a speed of 1 m/min or 4 m/min.

ii) All connections between the horn and the fixed installations are disconnected pneumatically; namely,
   - the eight electrical power connectors between horn end-plate and stripline;
   - the hollow piston for the cooling system;
   - the Lemo connector for the magnetic probe in the horn.

---

*) Gummi-Maag, Zurich.

iii) Pneumatic pistons unlock the two locking clamps of the horn chassis after positioning on the platform.

iv) After the target has been withdrawn from the horn and the biological iron shield moved away, the crane picks up the horn, transports it to its storage carriage (∿ 20 m upstream), then picks up the selected spare horn and brings it into position in the beam. Pneumatic pistons centre the horn automatically. These push the V-shaped ends of the alignment plates forward and sideways against centring rods, accomplishing a reproducible alignment precision of ±0.2 mm. Pneumatically operated locking clamps fasten the horn in this position.

v) Reconnection of the electrical and cooling systems, and the re-installation of the target and the biological shield complete the exchange cycle.

A complete exchange cycle takes approximately 20 minutes.

7. ELECTRICAL CHARACTERISTICS OF THE HORN SYSTEM

The electrical characteristics of the horn system are determined by the physical size of horn, stripline, connectors, and HT cables; their total inductance, ohmic resistance, and the characteristics of the power supply determine the shape of the current pulse produced by the discharge of the 13 capacitor units (forming the pulsed power supply).

7.1 Inductance

The inductance of the horn is calculated in the program INDUCT by subdividing the horn into 23 coaxial cones and using as formula for the inductance of each section:

$$L_i[\mathrm{nH}] = 50\,\ell_i \left[1 + 4\left(\frac{D_{i+1}\ln D_{i+1} - D_i \ln D_i}{D_{i+1} - D_i} - \frac{R_{i+1}\ln R_{i+1} - R_i \ln R_i}{R_{i+1} - R_i}\right)\right] , \qquad (10)$$

where D, R, and ℓ, measured in m, are the radius of the outer and inner conductors and the section length, respectively. Equation (10) was obtained by integrating the well-known formula for coaxial cylinders in the high-frequency range:

$$L_i = 200\, l_i \ln \frac{D_i}{R_i} . \qquad (10')$$

The sum of the inductances of the 23 sections gives a total inductance of 1020 nH for the horn.

The inductance of the stripline is calculated from

$$L_{str}[\mathrm{nH}] = \frac{4\pi\, s}{w}\,\ell = 267\ \mathrm{nH} , \qquad (11)$$

where ℓ is the length, w is the width of the stripline, and s is the distance between the conductor plates; all measurements are in centimetres. Taking into account the inductance of the polarity changer (30 nH), of the set of four pairs of electric power connectors (120/4 nH), and of the endplates and cableplates, the total inductance of the horn system amounts to L_{tot} = 1.4 μH.

7.2 Resistance

The program INDUCT also calculates the ohmic resistance of the inner and outer conductors, assuming a skin depth of 1.6 mm in Al for a 2.5 kHz sinusoidal pulse, and taking as specific electrical resistance κ_{spec} the values listed in Table 2. The ohmic resistance of the horn is found to be $R_H = 0.35$ mΩ.

Together with the ohmic resistance of the stripline, $R_{str} = 1.2$ mΩ, the total resistance of the horn system -- neglecting contact resistances -- is $R_{tot} = 2.2$ mΩ. This also includes the resistances of the connectors, connector plates, and polarity changer.

7.3 Resulting current pulse

The horn current pulse obtained by an overdamped discharge of the capacitor bank[4] ($C_{bank} = 280$ μF), has the typical form shown in Fig. 7, the non-sinusoidal part being due to the damping by a crowbar discharge and the horn system-resistance.

The sinusoidal pulse length (half wavelength) τ is given approximately by Thomson's equation:

$$\tau \approx \pi \sqrt{L_{tot}\, C_{bank}} \approx 200 \ \mu\text{sec} .$$

The pulse height is nominally 500 kA (12 kV; 13 discharge units). Two of the horns are designed for 400 kA pulses. The third one, which has a minimum thickness inner conductor, is designed for 340 kA.

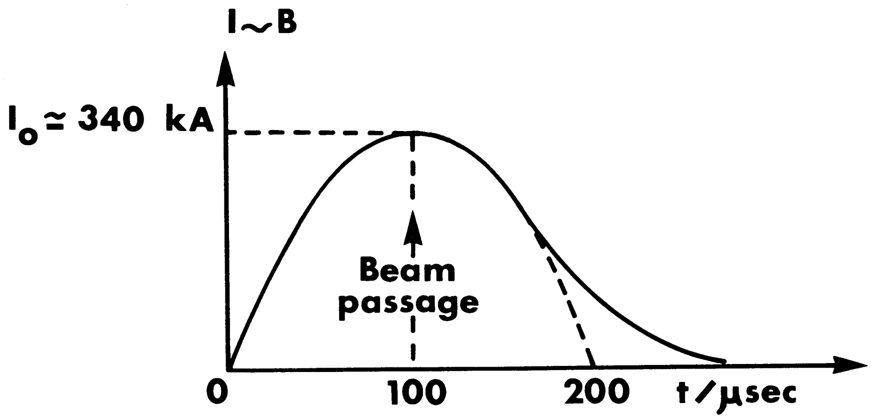

Fig. 7 Typical horn current form

8. MONITORING DEVICES AND TARGET SUPPORT

The pulse height of the current pulses during the beam passage is monitored by a magnetic pick-up coil[12] and recorded in a Hewlett Packard 2115 computer. The calibrated coil is inserted between the inner and outer conductors of the horn and measures via an integrator the magnetic flux B, which can be converted into the horn current by Eq. (1), with a precision of better than 2.2%. Simultaneously, the timing of current pulses can be checked with an accuracy of ±3 μsec, corresponding to relative current variations in the peak region of ±0.1%.

The highly radiation-resistant (> 10^9 rad) polymide Vespel*), which also has excellent electrical insulation and mechanical properties, has been used to protect the coil from the 10 kV horn potential.

The position of the proton beam is monitored by a set of five thermocouples, a secondary emission monitor[13] ("Budal"), and a television camera observing a ZnS scintillation screen immediately in front of the target. A similar set of four thermocouples and a Budal monitor $\sim$ 1 m further upstream allows the incident angle of the primary proton beam to be measured. The ZnS screen is useful for a quick, rough check of the beam position, whereas the Budal monitor serves for fine adjustments. The four thermocouples around the theoretical beam axis indicate the direction of eventual beam displacements, while thermocouples on beam axis are used for monitoring and maximizing the proton intensity.

A fast-ejected 26 GeV/c proton beam (1.5×10^{12} protons per pulse) heats up a 0.5 mm Ø thermocouple to an equilibrium temperature of $\sim$ 40°C above the ambient temperature.

In order to maximize proton absorption in the target, the 90 cm long target and its support can be inclined in any direction with a maximum angle of 3 mrad, keeping the target front end in the same position. For this purpose and to avoid the transmission of horn shock-vibrations to the fragile target, the target is suspended in a 50 cm long cone of 200 μm thick Mylar foil. The alignment inside the cone is better than ±0.1 mm. At the same time, this support keeps the target on floating electrical potential rather than on the HT potential of the horn. The Mylar is radiation-resistant only up to $\sim 2 \times 10^8$ rad, but has the advantage over Kapton of being easily ultrasonic-welded or glued by Araldite.

9. PERFORMANCE

The magnetic horn system has been tested in detail and has already completed the first stage (500,000 pictures in Gargamelle) of the present CERN neutrino experiment. During the course of this experiment an asymmetry in the distribution of muons in the neutrino shielding indicated that there could be a magnetic field asymmetry inside the horn. Recent measurements of the magnetic field[14] have shown that there is indeed an up-down asymmetry of a few per cent (zero near the neck, $\sim$ 2% half way along, and $\sim$ 9% at the downstream end of the horn) with a smaller (maximum 0.5%) left-right asymmetry. Features of this nature make it increasingly more difficult to determine the neutrino spectrum in Gargamelle from the observed muon distribution in the shielding. The magnetic field asymmetry was probably due to the fact that the current pulse was applied asymmetrically to the horn at the downstream end (Fig. 2), and as a consequence a more symmetrical current feeding has been tried[15]. These measurements (made at 130 kA instead of the usual 340 kA) show an over-all asymmetry of less than 1%, which can be explained by the mechanical tolerances of the concentricity of the two conductors. One of three available horns (the 340 kA version) broke owing to a weak welding line; the others have successfully passed long endurance tests (up to 8.5×10^5 pulses) at 340 kA and very short periods at 380 kA. The polarity changer has operated successfully in both polarities for more than 5×10^5 pulses at 340 kA.

The lamellae in the electric power connector have been changed in preventative maintenance after 2.5×10^5 pulses although no visible damage could be observed; however, the supplier suspects that fatigue effects spoil the elasticity qualities.

*) Du Pont de Nemours, S.A.

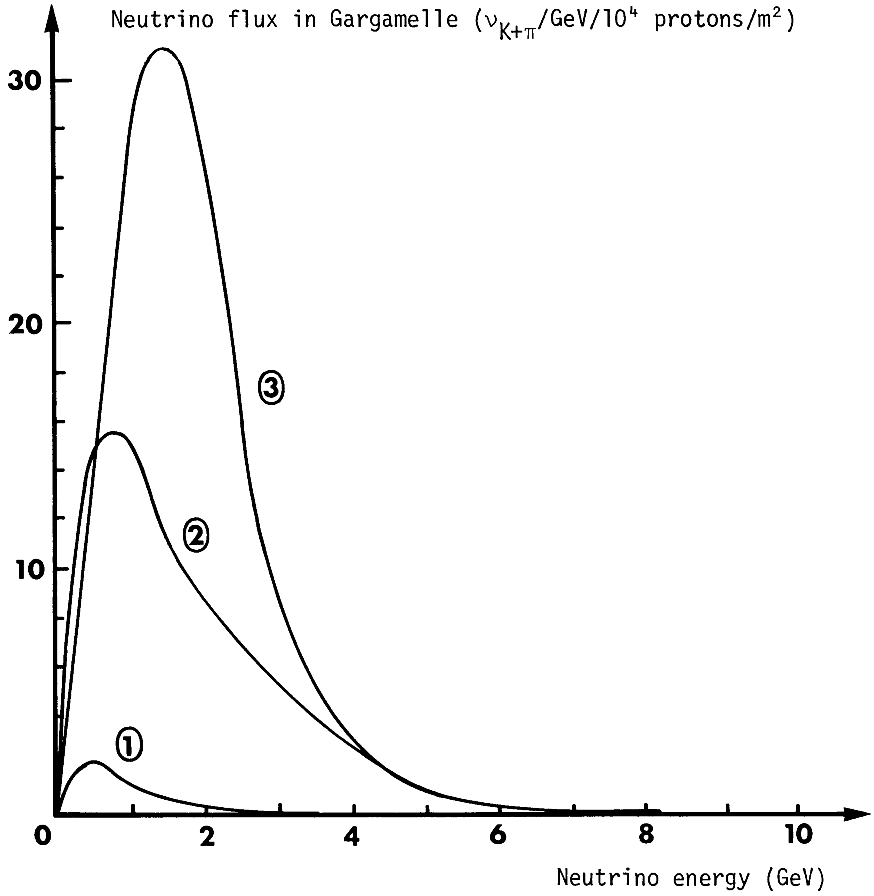

(1) Without focusing elements

(2) Horn only 340 kA

(3) Horn and reflectors 340 400 400 kA respectively

Fig. 8 Neutrino spectrum in the bubble chamber, calculated from the thermodynamical model (proton momentum: 26 GeV/c)

The neutrino spectrum in Gargamelle resulting from 26 GeV/c protons has been calculated by the NUFLUX program, using the 10-parameter formula for pion-kaon production, the actual dimensions of the present magnetic horn (340 kA version) and the parameters used in the neutrino experiment (Fig. 8). Compared to similar calculations for the 1967 horn we found a 10% enhancement of the neutrino spectrum in the energy range 1.5 to 4.0 GeV.

10. PROSPECTS AND SUGGESTIONS

10.1 Coaxial stripline and power connectors

Further development of the horn system will certainly need an investigation of higher radiation-resistant materials.

The present stripline, for instance, would not be adequate for radiation doses much higher than $\sim 2 \times 10^8$ rad. For neutrino experiments using the Booster or the 300 GeV/c Proton Synchrotron, the Mylar foils would have to be replaced several times during a run.

(Kapton foils, which are much more radiation-resistant, are too brittle for this purpose). Furthermore, the inductance of a sandwich-stripline is unnecessarily high, giving a 25% voltage drop along the stripline.

We therefore propose a new line consisting of 10 "conductors" in parallel, each of them consisting of two coaxial Al pipes of ≤ 10 m length, separated by a 3 mm thick insulating pipe of machined or cast highly radiation-resistant material. The outer diameter of such a conductor could be ∿ 6 cm, and the centre could be used for forced-air cooling if necessary.

The advantages of such a coaxial line, apart from its radiation resistance, would be:

- only a few per cent of the electromagnetic forces acting on the present stripline would be present (moreover, these would be symmetrical forces, which are easy to deal with);
- the inductance of the line would be only 80 nH instead of 270 nH, so that the pulse voltage could be lowered by ∿ 2 kV. This would reduce the risk of breakdown in the power supply, stripline, or horn, and would result in longer lifetimes of components and a saving of electrical power;
- since only ∿ 34 kA would flow through each conductor, heating would be minimal;
- a leak in the horn water-cooling system would no longer be a disaster since each conductor is a closed unit.

A coaxial electric power connector -- also remotely controlled by a pneumatic piston -- has been developed and successfully tested at 170 kA, 9 kV, over 80,000 pulses. The inductance of a system of four of these connectors would be only 10 nH as opposed to 30 nH for the present system. The insulator was a 5 mm thick layer of fibre-glass reinforced Araldite F905.

An advantage of reducing the total inductance is that the pulse length and therefore the mechanical stress on the inner conductor of the horn are reduced. A 10% shorter pulse length would result in 2.5% lower stress.

10.2 Simpler horn cooling

Assuming that future neutrino experiments at high energies (300 GeV) probably imply a lower repetition rate than at present (i.e. < 1 pulse/2 sec), a continuous forced-air cooling rather than pulsed-water cooling could possibly be employed. A preliminary test with a compressed air flow at 4 atm pressure through the present water pipes showed that an equilibrium temperature of 100°C in the neck region of the inner conductor was reached at 200 kA and a repetition rate of 1 pulse/2 sec. It seems that this temperature limit (mainly determined by the Araldite support in the neck region) would not be surpassed at 340 kA and a repetition rate of 1 pulse/4 sec, provided that a specially designed air jet system is used. This would result in a much simpler cooling system requiring less maintenance.

10.3 Target

For experiments with higher proton energies the target would probably be much further in front of the horn than it is at present. This would facilitate the optimization of target positioning in the beam, since thermocouples could be mounted directly onto the target as there would not be any risk of sparking between the horn and the target. Maximum target temperature would correspond to maximum proton absorption and therefore optimum target position.

Forced-air cooling would be necessary in order to keep the target temperature sufficiently low at higher proton intensities. With the present proton intensity of $\sim 1.5 \times 10^{12}$ ppp, the target temperature, extrapolated from tests, is already $\sim$ 130°C without cooling.

10.4 Reduction of particle absorption in air

For neutrino beams at the 300 GeV/c accelerator, the decay path for pions and kaons would be of the order of 600 m, which is approximately equal to one absorption length λ in air at normal pressure. The neutrino flux could be increased by $\sim$ 40% by having vacuum or at least a light (and inert) gas (e.g. helium, λ = 2500 m) instead of air in the decay path. It is therefore proposed to have a light plastic bag filled with 1 atm of He between the horn and reflector R2; this could be a $\sim$ 60 m long balloon made from commercially available "Polyurethane" which is -- as we have tested -- sufficiently radiation-resistant. The remainder of the tunnel could be either filled with similar He balloons or made vacuum-tight by means of plastic or metal tubes equal to the tunnel diameter. Owing to the finite window thickness, the effect of multiple Coulomb scattering on the particles is small: The r.m.s. projected scattering angle for pions or kaons of 80 GeV/c momentum (neutrino energy of $\approx$ 40 GeV) in a 2 cm thick Al plate is $\langle\theta\rangle \approx 0.04$ mrad. Nevertheless, windows should not be positioned too far upstream.

10.5 Other focusing possibilities

Other possible focusing devices -- such as toroidal coils, a (super-conducting) long, heavy current-carrying wire along the beam axis, a plasma[16)] and a wire lens[17)] -- have been studied, mainly for their optical properties. However, only the plasma lens promises better focusing qualities than a horn when used in beams with primary momenta greater than $\sim$ 50 GeV/c. The technical difficulties encountered in Brookhaven when using a 1.5 m long plasma lens give an idea of the problems to be solved when constructing a 5 m long plasma lens of 5-7 cm plasma radius and 400 kA current, which would be necessary to improve on the properties of an equally long horn. Even better optical properties could be obtained from a conical-shaped plasma lens if this were feasible. Standard focusing of the pion/kaon beam by a set of quadrupoles would result in a considerable loss in neutrino flux in the detector, but would have the advantage of a more straightforward narrow-band neutrino spectrum.

Acknowledgements

We wish to thank Dr. C.A. Ramm and Dr. H. Wachsmuth for encouraging the "magnetic horn" project, and Prof. A. Rousset for his interest and stimulation.

The untiring efforts of Mr. J. Gardies and Mr. R. Boulinguez in the construction and design of the horn, and Mr. J.M. Boban and Mr. D. Mouraux for the remotely-controlled overhead crane design are gratefully acknowledged.

We are grateful to Mr. M. Van Gulik for the calibration of the magnetic pick-up coil, to Mr. M. Van de Voorde for the radiation tests of various materials and to the CERN West Workshop for constructing the horn inner conductors. The personnel of the TC-L Beam Transport Group are thanked for providing their assistance during the operation of the horn.

REFERENCES

1) S. Van der Meer, CERN 61-7 (1961).

2) M. Giesch, B. Kuiper, B. Langeseth, S. Van der Meer, D. Neet, G. Plass, G. Pluym and B. de Raad, Nuclear Instrum. Methods 20, 58 (1963).

3) J.B.M. Pattison, The CERN neutrino beam, Proc. of the Neutrino Meeting, CERN (Jan. 1969), CERN 69-28, p. 13.

4) G. Gruber, R. Grüb and B. Langeseth, CERN-NPA/Int. 69-13 (1969).

5) A. Ašner and Ch. Iselin, CERN 66-24 (1966).

6) W. Venus, CERN computer program NUFLUX, unpublished.

7) G. Ziebarth, CERN-NPA/Int. 69-14 (1969).

8) G. Ziebarth, CERN-NPA/Int. 69-19 (1969).

9) O.W. Eshbach, Handbook of Engineering Fundamentals, 2nd edition (Wiley and Sons, Inc., NY, 1952), Section 5, p. 55.

10) R.C.A. Brown, CERN-TC, private communication.

11) M. Giesch, CERN-SI, private communication.

12) P. Actis and G. Ziebarth, CERN-TCL/Int. 71-9 (1971).

13) K. Budal, CERN 67-17 (1967).

14) J.C. Dusseux and J.M. Maugain, CERN-TCL/Int. 71-10 (1971).

15) J.C. Dusseux, R. Grüb and J.M. Maugain, CERN-TCL/Int. 72-2 (1972).

16) E.B. Forsyth, L.M. Lederman and J. Sunderland, The Brookhaven-Columbia plasma lens, Proc. of the Informal Conf. on Experimental Neutrino Physics, CERN (Jan. 1965), CERN 65-32, p. 131.

17) D. Luckey, Rev. Sci. Instrum. 31, 202 (1960).